PAPER

Dynamic modeling of dielectric elastomer actuators with a minimum energy structure

IOP Publishing Smart Materials and Structures
Smart Mater. Struct. **28** (2019) 085039 (10pp) https://doi.org/10.1088/1361-665X/ab2c1f

Dynamic modeling of dielectric elastomer actuators with a minimum energy structure

Jiang Zou[1,2] **and Guoying Gu**[1,2]

[1] Soft Robotics and Biodesign Lab, Robotics Institute, School of Mechanical Engineering, Shanghai Jiao Tong University, Shanghai, People's Republic of China
[2] State Key Laboratory of Mechanical System and Vibration, Shanghai Jiao Tong University, Shanghai, People's Republic of China

E-mail: guguoying@sjtu.edu.cn

Received 25 March 2019, revised 2 June 2019
Accepted for publication 24 June 2019
Published 23 July 2019

Abstract

Dielectric elastomer actuators with a minimum energy structure (DEAs-MES) have been widely used in developing different soft robotics, owing to their large strain and simple structure. However, there is rare study on dynamic modeling of DEAs-MES because of both geometric and viscoelastic nonlinearities. In this work, we present a dynamic modeling approach for DEAs-MES by using an equivalent slider-crank mechanism, where geometric nonlinearity is simplified for calculating the stress distribution on DEAs-MES and the viscoelastic nonlinearity is represented by a series of viscoelastic units. In this sense, the Lagrange equation can be utilized to obtain the analytical dynamic model of DEAs-MES. The quantitative comparisons between experimental data and predicted results well demonstrate the effectiveness of the development, where the maximum root-mean-square errors are less than 10.78%. This work presents the early attempt to analytically characterize the dynamic response of DEAs-MES, which will be necessary for further dynamic-model based control design in the field of soft robotics.

Keywords: Dielectric elastomer actuators, Minimum energy structure, Dynamic modeling approach, Geometric nonlinearity, Viscoelastic nonlinearity, Equivalent slider-crank mechanism

(Some figures may appear in colour only in the online journal)

1. Introduction

Dielectric elastomer actuators with a minimum energy structure (DEAs-MES) are a kind of promising configurations, which are fabricated by a pre-stretched dielectric elastomer membrane and a flexible frame. After releasing the pre-stretches, part of the stored strain energy in the dielectric elastomer membrane can be transferred into the flexible frame to reach an equilibrium state, resulting in the saddle-shape minimum energy structure [1, 2]. By employing a voltage to a DEA-MES, the expansion of the dielectric elastomer membrane leads to a new equilibrium state of the structure. Based on this simple working principle, DEAs-MES have been widely used to develop diverse soft devices and robots, including grippers [3, 4], climbing robots [5], crawling robots [6, 7], swimming robots [8] and flying robots [9].

However, there is still rare study to characterize the dynamic response of the DEAs-MES. The main difficulty relies on two kinds of nonlinearities, i.e. geometric nonlinearity [10] and viscoelastic nonlinearity [11]. The geometric nonlinearity is mainly caused by the calculation difficulty of the stress distribution on the saddle-shape structure. Although finite element methods have been widely adopted to investigate the stress distribution, they cannot provide an analytical model and usually require time-consuming calculations [12, 13]. Alternatively, some efforts have made to simplify the complex geometry. For example, by simplifying the saddle-shape structure to a rectangle planar, Shea *et al* [14] proposed an analytical modeling method for a DEA-MES to investigate the relationship between main geometric parameters and performance of the DEA-MES. In addition, Li *et al* [15] developed a pseudo-rigid-body model to qualitatively describe a DEA-MES

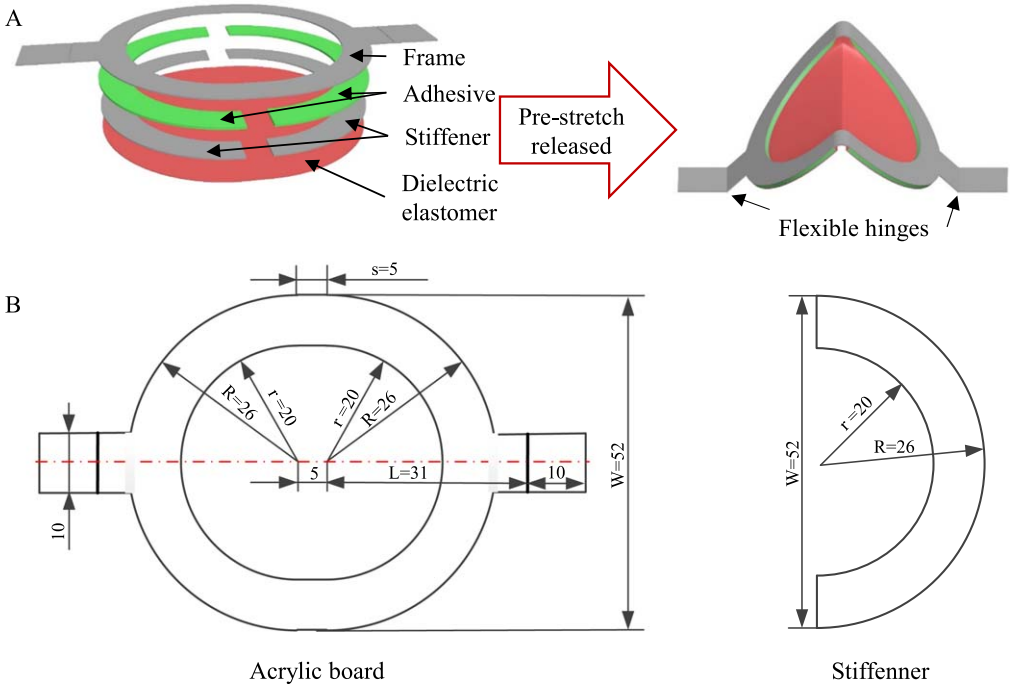

Figure 1. Schematic of the DEA-MES. (A) Structure of the DEA-MES; (B) Geometric parameters of the frame and stiffener (Unit: mm).

by using an equivalent nonlinear spring. However, these reported models usually ignore the viscoelasticity of the dynamic responses in DEAs-MES. By taking the viscoelastic nonlinearity into consideration, Cao *et al* [16] proposed a dynamic model to describe the dynamic response of the DEA-MES, but it ignored the geometric nonlinearity.

Therefore, this work is motivated to present a dynamic model for the DEA-MES by taking both geometric and viscoelastic nonlinearities into consideration. Our dynamic model is developed as: Firstly, a constitutive model is established to calculate the stress distribution on the DEA-MES by simplifying the geometric nonlinearity of the DEA-MES. Then, the DEA-MES is equivalent to a slider-crank mechanism with a series of viscoelastic units that is used to represent the viscoelastic nonlinearity of the DEA-MES.

Finally, a dynamic model is established based on the Lagrange equation. To verify the effectiveness of the developed dynamic model, different experiments are conducted under different exciting voltages with a frequency range of 1.0–10.0 Hz. The comparisons of experimental data and predicted results demonstrate that our dynamic model can quantitatively describe the dynamic response of the DEA-MES, including slow-time viscoelastic creep nonlinearity and rate-dependent viscoelastic hysteresis nonlinearity, with maximum root-mean-square errors less than 10.78%. The main contribution of this work depends on the fact that: an analytic model is proposed for dynamic description of the DEA-MES in a wide frequency range, which is the first time for dynamic modeling of the DEA-MES.

The structure of the remainder paper is organized as follow. Section 2 introduces the fabrication of the DEA-MES, the experimental platform and observations. Section 3 describes the development of the dynamic model. The identification and verification of the developed model are detailed in section 4 Section 5 concludes this paper.

2. Results

2.1. Actuator fabrication

In this work, a DEA-MES shown in figure 1(A) is designed for proof-and-concept testing. To fabricate the DEA-MES, seven steps are involved: (i) a laser cutting machine is adopted to manufacture a frame (acrylic board, thickness 0.3 mm) with two flexible hinges; (ii) two laser cutting stiffeners (acrylic board, thickness 0.3 mm) are adhered to the frame by 3 M VHB 4905 (thickness 0.5 mm), which separate the frame into two parts in terms of the stiffen part and weak part; (iii) a dielectric elastomer membrane (3 M VHB 4910, thickness 1.0 mm) is pre- stretched by 5 × 5 and then kept for 12 h to make it stable; (iv) the frame is adhered to the pre-stretched dielectric elastomer membrane; (v) carbon grease (MG Chemical 846-80 G) as compliant electrodes is used to coat both sides of the dielectric elastomer membrane; (vi) after releasing the pre-stretch, the DEA-MES forms a saddle-shape; (vii) two soft wires are used to connect the actuator to a high voltage amplifier. The geometric parameters of the frame and the stiffener are provided in figure 1(B).

Figure 2 shows the illustration of the working principle of the DEA-MES. At the reference state, the DEA-MES has a length of l_0 and an angle of θ_0. At the actuation state, when the exciting voltage of the DEA-MES increases, the l_0 increases to l and the θ_0 decreases to θ. When the exciting voltage decreases to zero, the DEA-MES recovers to the reference state. As a result, the DEA-MES can generate a periodic movement under a periodic exciting voltage.

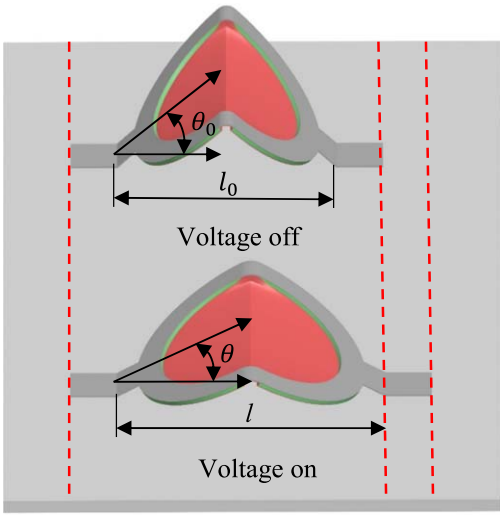

Figure 2. Working principle of the DEA-MES.

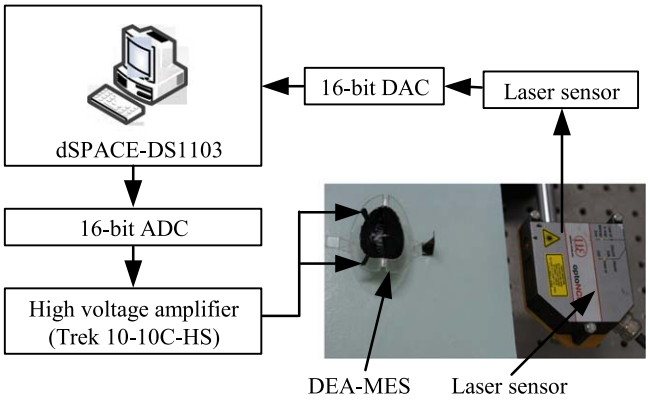

Figure 3. Experimental platform for testing the fabricated DEA-MES.

2.2. Actuator testing

In this section, we build an experimental platform shown in figure 3 to test the fabricated DEA-MES. Our experimental platform consists of a high voltage amplifier, a laser sensor and a control module. The high voltage amplifier (TREK 10/10C-HS) with a fixed gain of 1000 is used to provide exciting voltages for the DEA-MES. The real-time output displacement is recorded by the laser sensor (Micro-Epsilon ILD2300-100, range of 100 mm with an analogue output 0-10 V). The control module dSPACE-DS1103 board, equipped with 16 bit analogue-to-digital converters (ADCs) and 16 bit digital-to-analogue converters (DACs), is utilized to generate control signal for the high voltage amplifier and capture the displacement signal form the laser sensor. In this work, the sampling time is set to be 1 ms. In addition, we should note that: when the amplitude of the exciting voltage exceeds 6 kV, some failure phenomena (such as wrinkle [17, 18]) can be observed. Therefore, the maximum amplitude of the exciting voltage is limited to 5 kV in the following experiments. In addition, the minimum voltage is 0.5 kV to satisfy the lowest exciting voltage.

2.3. Experimental results

In this section, a series of experiments are conducted to investigate the dynamic responses of the DEA-MES. To this end, sinusoidal exciting voltages with different frequencies and amplitudes are adopted to excite the DEA-MES, in the form of:

$$V(t) = \frac{A - 0.5}{2}\sin(2\pi ft - 0.5\pi) + \frac{A + 0.5}{2}(\text{kV}), \quad (1)$$

where A and f represent the amplitude and frequency of the exciting voltage, respectively. The measuring process involves three steps: (i) one end of the DEA-MES is fixed on the ground and let the other one be free; (ii) the $V(t)$ is applied to the DEA-MES and the output displacement is recorded by the laser sensor; (iii) after at least 50 exciting periods, the measurement is stopped.

Figure 4(A) shows one example of the exciting voltage when the amplitude and frequency equal to 5 kV and 1 Hz, respectively. The real-time output displacement is plotted as a function of time and the exciting voltage as shown in figures 4(B) and (C), respectively. In addition, figure 4(D) shows the comparisons of viscoelastic hysteresis loops under different frequencies. From the experimental results, we can observe that:

(i) The time-domain dynamic response (figure 4(B)) can be separated into two regions: transition region and stable region. During the transition region, the output displacement shows a slow drift phenomenon, generally due to the viscoelastic creep effect [19, 20]. The results show that the viscoelastic creep effect dominants the output displacement in the first few circles and then becomes ignorable during the stable region.
(ii) The viscoelastic hysteresis and creep effects are coupled during the transition region (figure 4(C)).
(iii) The viscoelastic hysteresis loops are both asymmetric and rate-dependent (figure 4(D)).

The above observations indicate that the dynamic responses of the DEA-MES are a nonlinear and non-equilibrium process and there is energy dissipated under periodic exciting voltages [11, 21]. In the following, we will develop a model to quantitatively describe these dynamic responses of the DEA-MES.

Remark. It should be mentioned that the critical value for dividing the displacement into two regions may be not unique, but it does not change the feature of the viscoelastic creep nonlinearity that is a slow-time effect.

3. Dynamic modeling

In this section, we firstly calculate the stress distribution on the DEA-MES, which is equivalent to a slider-crank mechanism with a series of viscoelastic units. Then, the Lagrange equation is adopted to analytically characterize the dynamic responses of the DEA-MES.

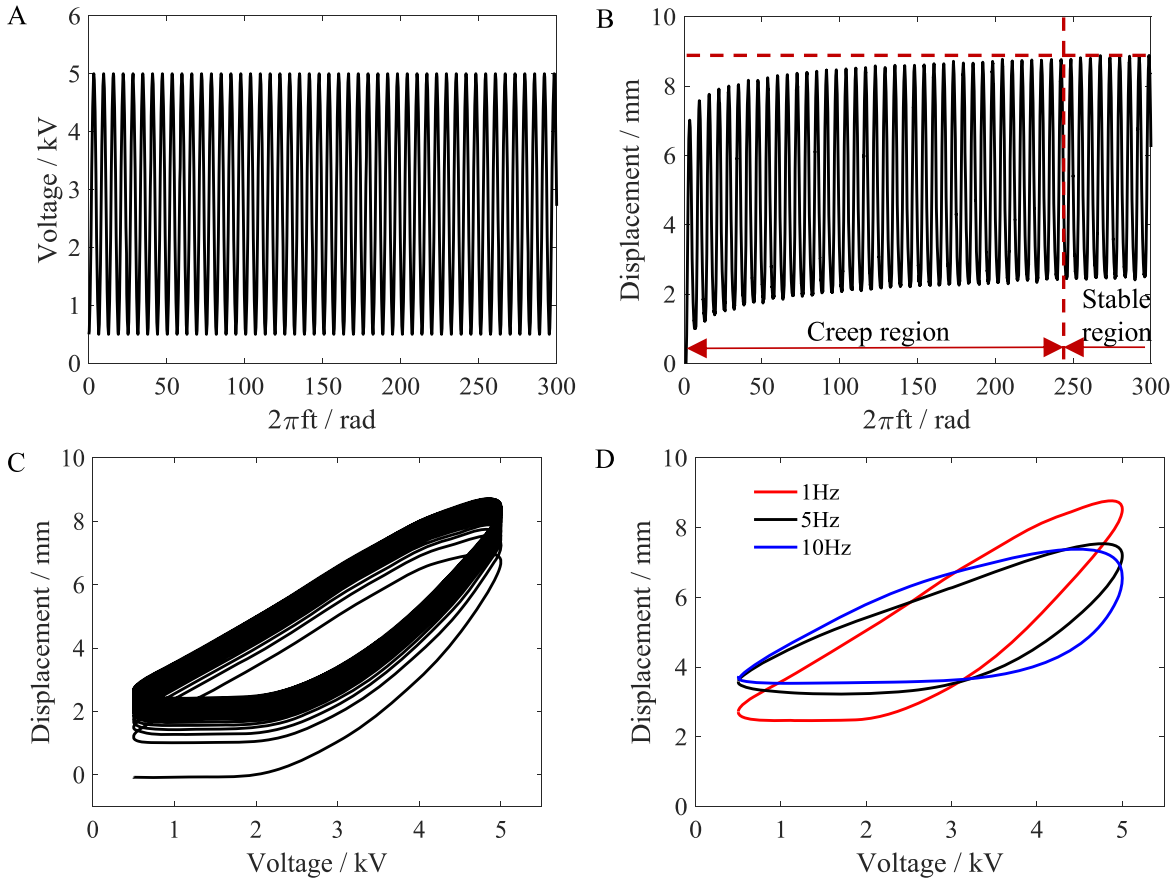

Figure 4. Experimental results of the DEA-MES with the sinusoidal voltage excitation. (A) The applied sinusoidal voltage is plotted as a function of time with a frequency of 1 Hz; (B) The output displacement is plotted as a function of time with a frequency of 1 Hz; (C) The output displacement is plotted as a function of exciting voltage with a frequency of 1 Hz; (D) The comparisons of viscoelastic hysteresis loops under different frequencies.

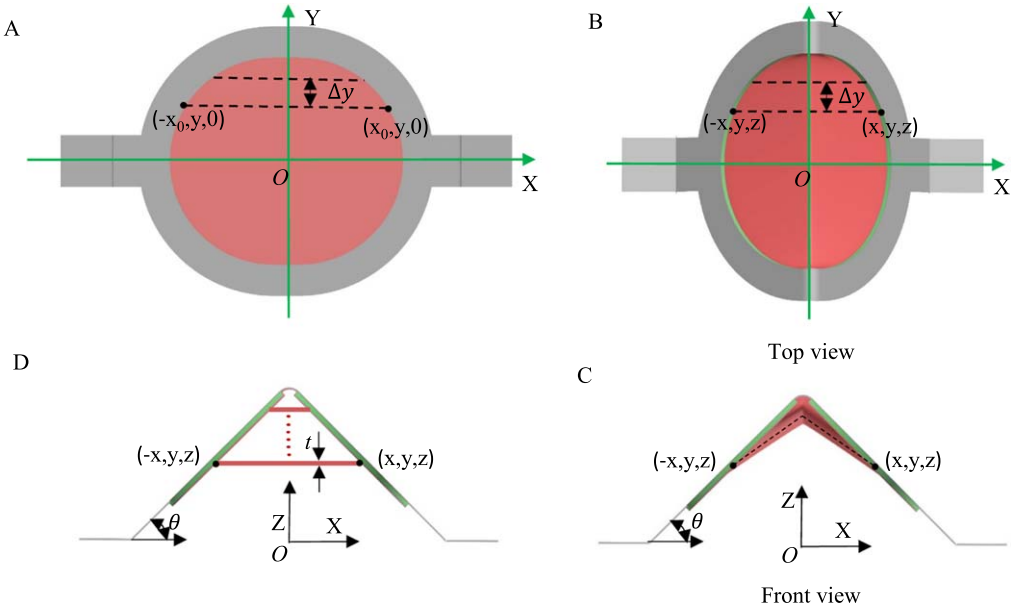

Figure 5. Calculating the stress distribution on the DEA-MES. (A) The dielectric elastomer membrane at the pre-stretched state; (B), (C) The top view and front view of the saddle-shape DEA-MES when the pre-stretches are released; (D) The saddle-shape DEA-MES is simplified to calculate the stress distribution.

3.1. Stress distribution calculation

For the convenience of describing, a Cartesian coordinate is established at the center of the DEA-MES. Considering a rectangular dielectric elastomer element (shown in figure 5) between two horizontal lines with Y-coordinates of y and $y+\Delta y$, at the pre-stretched state, its' initial length, width and thickness equal to $2x_0$, Δy and t_0, respectively. After releasing the pre-stretches, the dielectric elastomer element forms a complex saddle-shape (Top view in figure 5(B) and front view in figure 5(C)). To simplify the geometric nonlinearity, the element is modelled by a new rectangular dielectric elastomer element with a length of $2x$, a width of Δy and a thickness of t as shown in figure 5(D). Therefore, three relative stretches in the length, width and thickness directions can be defined as:

$$\begin{aligned}\lambda_{xr} &= \frac{x}{x_0} = \cos\theta \\ \lambda_{yr} &= \frac{\Delta y}{\Delta y} = 1 \\ \lambda_{zr} &= \frac{t}{t_0}.\end{aligned} \tag{2}$$

It should be noted that because the deformation of the DEA-MES in the Y direction can be ignored, the λ_{yr} always equals to 1. In addition, due to the incompressibility of the dielectric elastomers [21], the relative stretches should satisfy:

$$2x_0 \cdot \Delta y \cdot t_0 = 2x \cdot \Delta y \cdot t \Rightarrow \lambda_{xr}\lambda_{zr} = 1. \tag{3}$$

Taking the pre-stretches of the dielectric elastomer membrane into consideration, the total stretches can be expressed as:

$$\begin{aligned}\lambda_x &= \lambda_{xr}\lambda_{x0} \\ \lambda_y &= \lambda_{yr}\lambda_{y0} \\ \lambda_z &= \lambda_{zr}\lambda_{z0},\end{aligned} \tag{4}$$

where the initial stretches $\lambda_{x0} = \lambda_{y0} = 5$ and $\lambda_{z0} = 1/\lambda_{x0}\lambda_{x0} = 1/25$. Based on the stretches of the dielectric elastomer element, the corresponding free energy density W can be developed as the sum of deformation and electric energy, which can be given by:

$$W = \sum_{i=1}^{N} \frac{\mu_i}{\alpha_i}(\lambda_x^{\alpha_i} + \lambda_y^{\alpha_i} + \lambda_z^{\alpha_i} - 3) + \frac{D^2}{2\varepsilon_0\varepsilon_r}, \tag{5}$$

where the first part represents the Ogden model [23, 24] based deformation energy, the μ_i and α_i are material parameters of the dielectric elastomer. N represents the number of terms in the Ogden model. D is the charge density over the electrodes. ε_0 and ε_r are the vacuum permittivity and the relative permittivity, respectively. Substituting (2)–(4) into (5), we can obtain:

$$W = \sum_{i=1}^{N} \frac{\mu_i}{\alpha_i}(\lambda_{x0}^{\alpha_i}\lambda_{xr}^{\alpha_i} + \lambda_{y0}^{\alpha_i} + \lambda_{z0}^{\alpha_i}\lambda_{xr}^{-\alpha_i} - 3) + \frac{D^2}{2\varepsilon_0\varepsilon_r}. \tag{6}$$

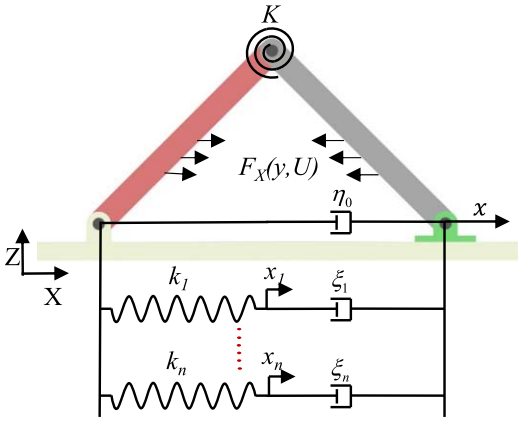

Figure 6. The DEA-MES is equivalent to a slider-crank mechanism.

Then, the stress σ_x in the X direction and actual electric field can be derived by differentiation (6) as below:

$$\begin{aligned}\sigma_x &= \lambda_{x0}\lambda_{xr}\frac{\partial W}{\partial(\lambda_{x0}\lambda_{xr})} - ED \\ E &= \frac{\partial W}{\partial D}.\end{aligned} \tag{7}$$

Substituting (6) into (7), the σ_x can be obtained as:

$$\sigma_x = \sum_{i=1}^{N}(\mu_i\lambda_{x0}^{\alpha_i}\lambda_{xr}^{\alpha_i} - \mu_i\lambda_{z0}^{\alpha_i}\lambda_{xr}^{-\alpha_i}) - \varepsilon_0\varepsilon_r\left(\frac{U\lambda_{xr}}{t_0}\right)^2, \tag{8}$$

where the U represents the exciting voltage. In addition, we would like to mention that due to the stress in the Y direction is vertical to the movement of the DEA-MES, it is unnecessary to calculate it. Based on the (8), we can further obtain the active force density between the dielectric elastomer membrane and the frame. For example, the active force density in the X direction can be expressed as:

$$F_X(y, U) = \frac{\sigma_x t_0 \Delta y}{\lambda_{xr}} \Big/ \Delta y = \frac{\sigma_x t_0}{\cos\theta}. \tag{9}$$

3.2. Establishing dynamic model

To model the dynamic responses, the DEA-MES is equivalent to a slider-crank mechanism shown in figure 6. Considering the viscoelasticity of the DEA-MES, a series of viscoelastic units are added. In addition, a coulomb damping is also introduced into the equivalent slider-crank mechanism to represent the air drag and frictions. Besides, we should mention that the mass of the dielectric elastomer membrane is ignored, because it is much lighter than that of the frame. Table 1 lists all the geometric parameters of the equivalent slider-crank mechanism. The K represents the bending stiffness of the frame, which can be written as:

$$K = \frac{E(W - 2r)t^3}{12s}, \tag{10}$$

where the E and t are the elastic modulus and the thickness of the acrylic board, respectively; W, r and s are three geometirc parameters of the acrylic board that are defined in figure 1(B).

Table 1. The geometric parameters of the equivalent slider-crank mechanism.

Symbol	Physical meaning	Value
l_m	Position of the mass center	15.78 mm
L	Length of the crank and connecting rod	33.50 mm
m_1	Mass of the crank and connection rod	0.603 g
m_2	Mass of the slider	0.40 g
J	Rotational inertia of the crank and connection rod	156.56 g mm^2

Table 2. The unknown parameters of the dynamic model.

Parameters	Symbol	Physical meaning
Material	ε_r	Relative permittivity
	N	The number of terms in the Ogden model
	α_i	Material constitutive parameters
	μ_i	Material constitutive parameters
Coefficient	n	The number of the viscoelastic units
	x_i	The deformation of the spring in the viscoelastic units
	k_i	The stiffness of the spring in the viscoelastic units
	ξ_i	The dashpot of the viscoelastic units
	η_0	The coulomb damping ratio

Table 3. The identified material parameters.

i	μ_i/kPa	α_i	ε_r	N
1	634.06	0.331	1.704	4
2	127.92	0.744		
3	73.98	0.243		
4	3.45	3.306		

Based on the equivalent slider-crank mechanism, Lagrange equation [22] is adopted to establish a dynamic model for the DEA-MES. In general, the Lagrange equation can be written as:

$$\frac{d}{dt}\left(\frac{dE_k}{d\dot{x}}\right) - \frac{dE_k}{dx} + \frac{dE_p}{dx} = F, \tag{11}$$

where the E_k and E_p represent kinetic energy and potential energy, respectively. x and F are generalized coordinate and force, respectively. To employ the Lagrange equation, we firstly select the angle θ as the generalized coordinate and then calculate the E_k, E_p and F of the DEA-MES. According to working principle (figure 2) of the DEA-MES, the positions of mass center of crank (x_{a1}, z_{a1}), connecting rod (x_{a2}, z_{a2}) and slider (x_{a3}, z_{a3}) can be expressed as:

$$\begin{aligned} x_{a1} &= l_m \cos\theta \\ z_{a1} &= l_m \sin\theta \\ x_{a2} &= 2l\cos\theta - l_m\cos\theta \\ z_{a2} &= l_m \sin\theta \\ x_{a3} &= 2l\cos\theta \\ z_{a3} &= 0. \end{aligned} \tag{12}$$

Then, we can obtain the velocity of the mass center as:

$$\begin{aligned} \dot{x}_{a1} &= -l_m \sin\theta\dot{\theta} \\ \dot{z}_{a1} &= l_m \cos\theta\dot{\theta} \\ \dot{x}_{a2} &= -(2l - l_m)\sin\theta\dot{\theta} \\ \dot{z}_{a2} &= l_m \cos\theta\dot{\theta} \\ \dot{x}_{a3} &= -2l \sin\theta\dot{\theta} \\ \dot{z}_{a3} &= 0. \end{aligned} \tag{13}$$

The total kinetic energy of the DEA-MES can be written as:

$$\begin{aligned} E_k &= \frac{1}{2}m_1(\dot{x}_{a1}^2 + \dot{z}_{a1}^2) + \frac{1}{2}J\dot{\theta}^2 + \frac{1}{2}m_1(\dot{x}_{a2}^2 + \dot{z}_{a2}^2) \\ &\quad + \frac{1}{2}J\dot{\theta}^2 + \frac{1}{2}m_2(\dot{x}_{a3}^2 + \dot{z}_{a3}^2) \\ &= \left\{ J + \frac{1}{2}m_1[(-2L + l_m)^2 \sin\theta^2 + l_m^2\cos\theta^2 \right. \\ &\quad \left. + l_m^2] + \frac{1}{2}m_2(-2L\sin\theta)^2 \right\}\dot{\theta}^2. \end{aligned} \tag{14}$$

In addition, the potential energy of the DEA-MES can be expressed as:

$$E_p = 2m_1 g l_m \sin\theta + \frac{1}{2}K(2\theta)^2. \tag{15}$$

According to the virtual work principle, we can obtain the F as:

$$\begin{aligned} F &= 2\sin\theta\int_{-r}^{r} F_X(y, U)xdy - \eta_0(2l\sin\theta)^2\dot{\theta} \\ &\quad - \sum_{i=1}^{n} k_i x_i \cdot (2l\sin\theta). \end{aligned} \tag{16}$$

The derivate of the kinetic and potential energy can be expressed as :

$$\begin{aligned} \frac{dE_k}{d\dot{\theta}} &= \{2J + m_1[(-2L + l_m)^2\sin\theta^2 + l_m^2\cos\theta^2 \\ &\quad + l_m^2] + 4m_2L^2\sin\theta^2\}\ddot{\theta}, \end{aligned} \tag{17}$$

$$\begin{aligned} \frac{d}{dt}\frac{dE_k}{d\dot{\theta}} &= \{2J + m_1[(-2L + l_m)^2\sin\theta^2 + l_m^2\cos\theta^2 \\ &\quad + l_m^2] + 4m_2L^2\sin\theta^2\}\ddot{\theta} \\ &\quad + [8m_1(L^2 - Ll_m) + 8m_2L^2]\sin\theta\cos\theta\dot{\theta}^2, \end{aligned} \tag{18}$$

$$\frac{\partial E_k}{\partial\theta} = [4m_1(L^2 - Ll_m) + 4m_2L^2]\sin\theta\cos\theta\dot{\theta}^2, \tag{19}$$

$$\frac{dE_p}{d\theta} = 2m_1 g l_m\cos\theta + 4K\theta. \tag{20}$$

Substituting (17)–(20) into (11), the dynamic model of the DEA-MES is obtained as:

$$\begin{aligned} &A\ddot{\theta} + B\dot{\theta}^2 + 2m_1 g l_m\cos\theta + 4K\theta = F \\ &k_i x_i = \xi(-2L\sin\theta\dot{\theta} - \dot{x}_i),\ i = 1, 2, \cdots n, \end{aligned} \tag{21}$$

where

$$\begin{aligned} A &= 2J + m_1[(-2L + l_m)^2\sin\theta^2 + l_m^2\cos\theta^2 \\ &\quad + l_m^2] + 4m_2L^2\sin\theta^2, \end{aligned} \tag{22}$$

$$B = [4m_1(L^2 - Ll_m) + 4m_2L^2]\sin\theta\cos\theta. \tag{23}$$

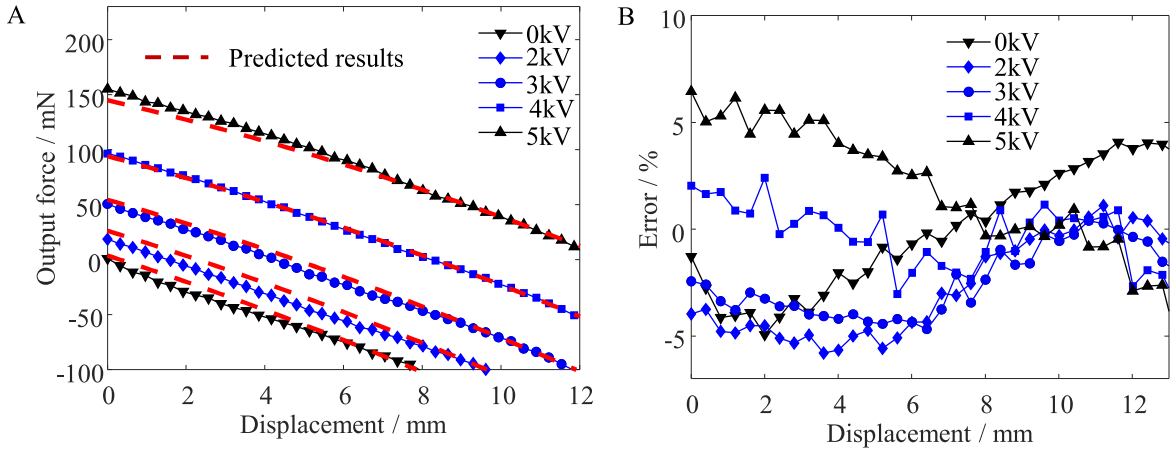

Figure 7. Material parameters identification. (A) The experimental data and predicted results are plotted as a function of the output displacement under different step voltages in the range of 0–5 kV (the experimental data in dark curve are used for material parameters' identification and the rest experimental data in blue are utilized to further verify the effectiveness of the material parameters); (B) The predicted errors under different step voltages.

Table 4. The identified coefficients of the viscoelastic units.

i	k_i(N m^{-1})	ξ_i(N s m^{-1})	η_0(N s m^{-1})
1	66	0.55	0.1
2	8	4	
3	3.5	20	
4	0.8	50	

In the (21)–(23), the geometric parameters are known parameters listed in table 1. The rest parameters are needed to be identified in the following section.

4. Dynamic model identification and verification

The unknown parameters of the dynamic model are listed in table 2, which can be separated into material parameters and coefficients of the viscoelastic units. The material parameters only influence the quasi-static response of the DEA-MES while the coefficients of the viscoelastic units only affect the dynamic response. Therefore, the material parameters are firstly identified by quasi-static responses and then the coefficients of the viscoelastic units are further identified based on dynamic response.

4.1. Model identification

To identify the material parameters, we firstly conduct a series of experiments to characterize the quasi-static responses of the DEA-MES under different step voltages (see [5] for more details about the experimental method). Then, the material parameters are identified by the genetic algorithm in the MATLAB optimization toolbox. To employ the genetic algorithm, we firstly choose a fitness function as:

$$GA = \min \sum [F - F^a]^2, \tag{24}$$

where the F and F^a represent the measured output force and predicted output force, respectively. In the identification, the number of terms in the Ogden model is set to be 4. The initial conditions of the genetic algorithm are listed below:

(i) The number of the variable is 9;
(ii) The bounds of the μ_i, α_i and ε_r are set as:

$$\begin{aligned} &1\ \text{kPa} \leqslant \mu_i \leqslant 1000\ \text{kPa} \\ &0 \leqslant \alpha_i \leqslant 5 \\ &0 \leqslant \varepsilon_r \leqslant 5 \end{aligned} \tag{25}$$

(iii) Population size and generation are set to be 100 and 1000, respectively;
(iv) The rest parameters of the genetic algorithm remain the default vales.

The identified material parameters are listed in table 3. The comparisons between the experimental data (0 and 5 kV, dark curves) and predicted results (0 and 5 kV, red curves) are shown in figure 7(A), and the predicted errors are plotted in figure 7(B). It can be seen that the model can precisely characterize the quasi-static responses of the DEA-MES. In addition, other three experimental results (2, 3 and 4 kV, blue curves in figure 7(A) and (B)) are further used for verification, which clearly demonstrates the effectiveness of the material parameters. And the maximum predicted errors are less than 6%.

With the identified material parameters, the coefficients of the viscoelastic units are further identified based on the dynamic responses of the DEA-MES. At first, we randomly choose three dynamic responses under different frequencies (for example, 1, 5 and 10 Hz in this work) as experimental data, then we manually tune the coefficients of the viscoelastic units to fit the experimental data with a frequency of 5 Hz. At last, we slowly tune the coefficients to balance the absolute maximum predicted errors under 1 and 10 Hz until they basically equal to each other. Based on this method, we get the coefficients of the viscoelastic units that are listed in table 4. The comparisons between experimental data and the predicted results are shown in figures 8(A)–(C) and the predicted errors are also illustrated in figure 8(D). It can be seen that the dynamic model can precisely describe the viscoelastic dynamic responses of the DEA-MES. To quantitatively

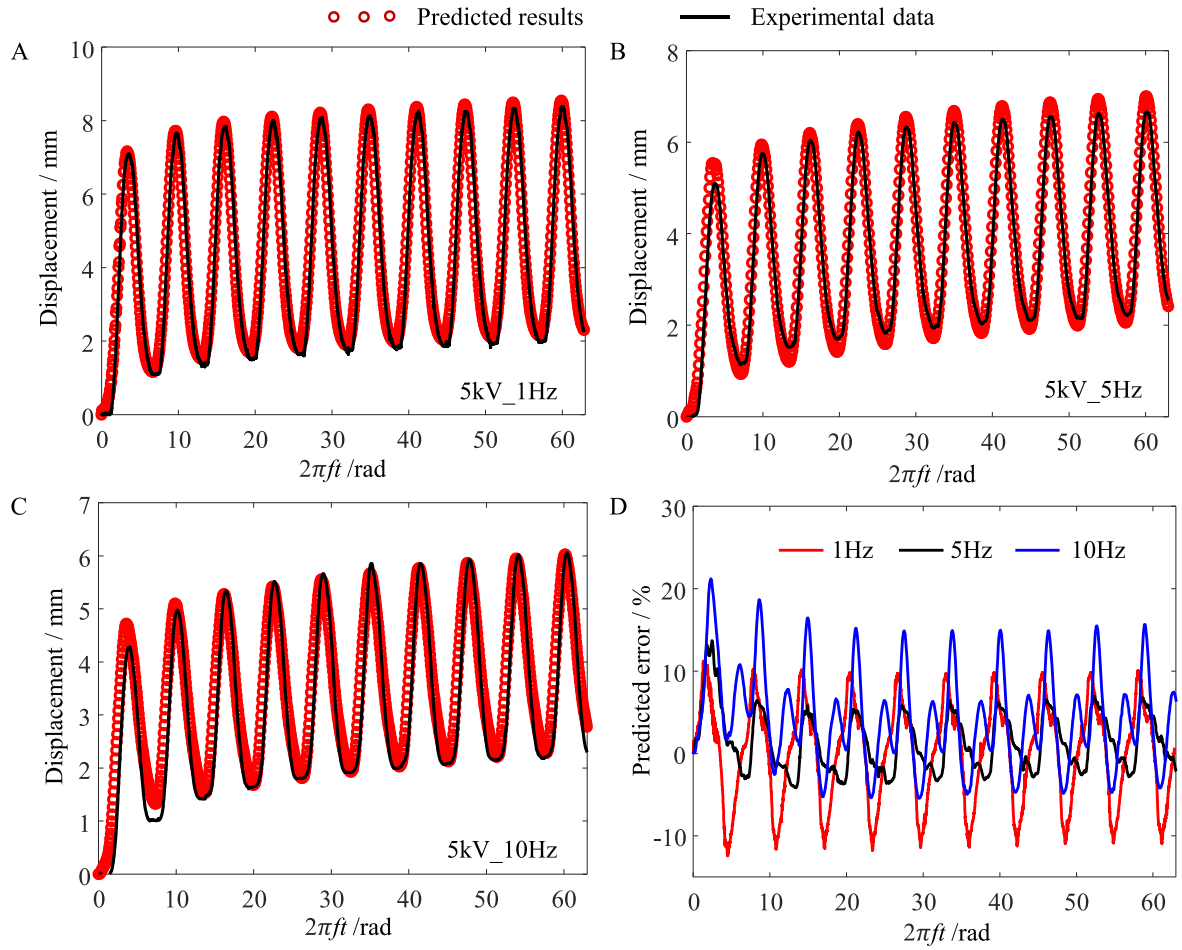

Figure 8. Dynamic model identification under different frequencies when the amplitudes exciting voltages equal to 5 kV. (A)–(C) The experimental data and predicted results are plotted as a function of the phase position under the frequency of 1, 5 and 10 Hz; (D) The predicted errors are plotted as a function of phase position.

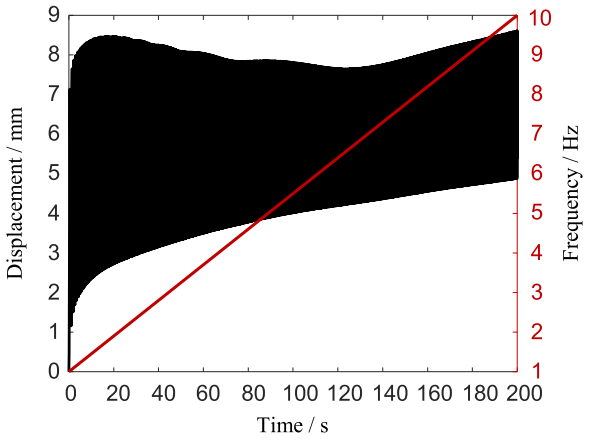

Figure 9. The predicted amplitude-frequency response of the DEA-MES.

describe the precision of the identified model, a root-mean-square error e_{rms} is defined as:

$$e_{rms} = \frac{\sqrt{\frac{1}{N}\sum_{i=1}^{N}[y(i) - y^a(i)]^2}}{\max(y^a) - \min(y^a)}, \quad (26)$$

where the y and y^a represent the experimental data and predicted results, respectively. N is the number of the experimental data. Then, we can obtain that the e_{rms} of 1 Hz, 5 Hz and 10 Hz are 6.14%, 3.88% and 7.37%, respectively. In addition, based on the dynamic model, we also can calculate the amplitude-frequency response of the DEA-MES that is shown in figure 9. It can be seen that the amplitude-frequency response is similar to the measured amplitudes under different frequencies. Therefore, the dynamic model can precisely describe the dynamic response of the DEA-MES when amplitude of the exciting voltage equals to 5.0 kV and the frequency is in the range of 1–10 Hz.

4.2. Model verification

To further verify the performances of our developed dynamic model, more experiments with different frequencies (1–10 Hz) and amplitudes (4–5 kV) are conducted. For example, figures 10(A)–(C) shows the comparisons between the experimental data and predicted results when the amplitude of the exciting voltage equals to 4 kV. The predicted errors are also provided in figure 10(D). In addition, the e_{rms} of 20 experiments are summarized in table 5. It can be

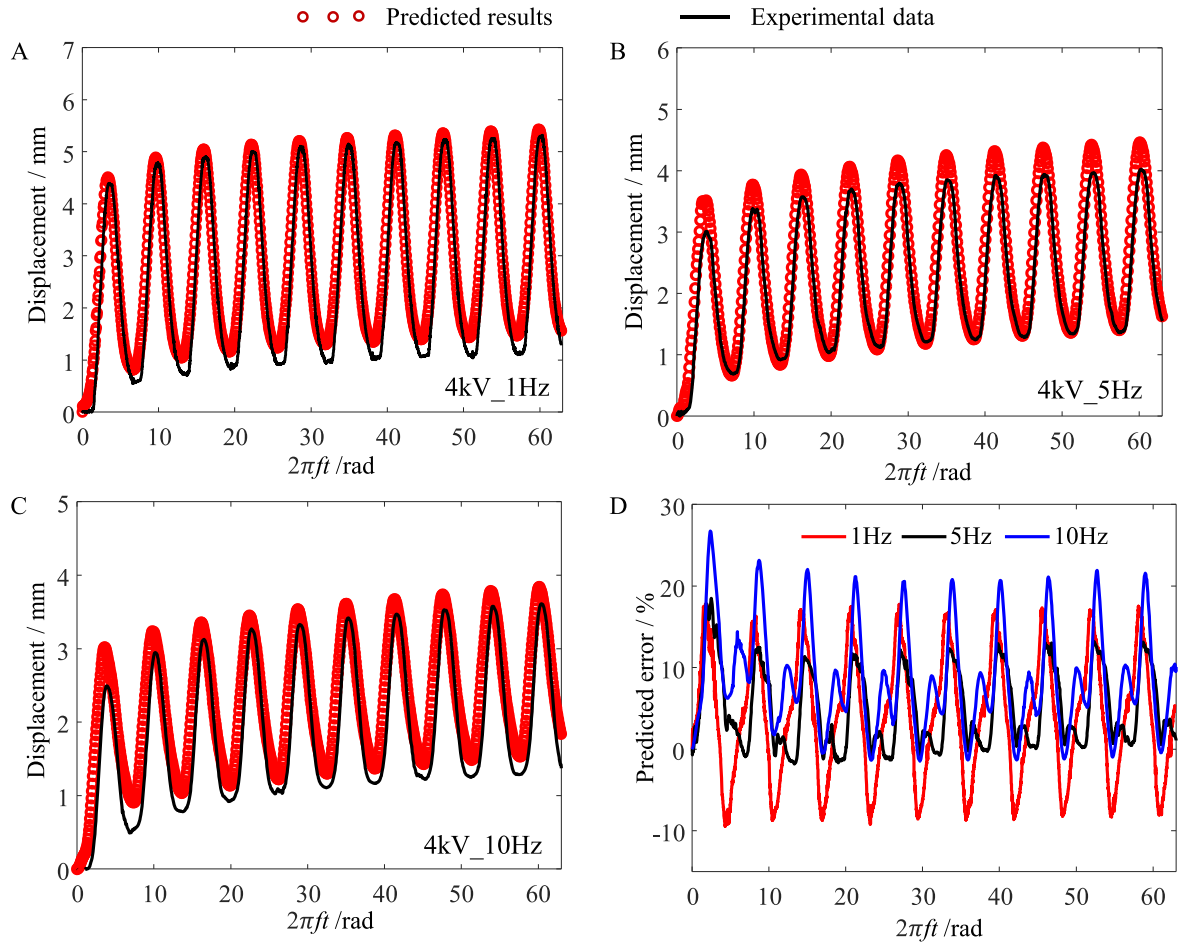

Figure 10. Dynamic model verification under different frequencies when the amplitudes of the exciting voltages equal to 4 kV. (A)–(C) The experimental data and predicted results are plotted as a function of the phase position under the frequency of 1, 5 and 10 Hz; (D) the predicted errors are plotted as a function of phase position.

Table 5. Predicted errors of the dynamcial model under different exciting voltages.

Predicted errors/%		
Frequency/Hz	Voltage/kV	
	5	4
1	6.14	8.67
2A	5.85	7.62
3	5.10	7.36
4	4.50	7.74
5	3.88	7.02
6	3.78	7.25
7	5.30	8.45
8	6.22	8.52
9	6.39	9.06
10	7.37	10.78

concluded that our dynamic model can precisely describe the viscoelastic dynamic responses of the DEA-MES when the frequency and amplitude of the exciting voltage are in the range of 1–10 Hz and 4–5 kV. And the maximum root-mean-square errors are less than 10.78%.

Remark. It should be mentioned that the main reasons of simplifying the DEA-MES to a slider crank mechanism depend on two facts: (i) they generate similar motions; (ii) it is convenient to adopt Lagrange equation for dynamic description of the DEA-MES. Of course, this method still can be applied to different DEAs-MES, while the main difference is that we need to identify the parameters based on the current experimental data. In addition, for other DEAs (such as a planar DEA or conical DEA), according to their motional features, it is better to simplify them to a spring-mass system rather than the slider-crank mechanism, but the Lagrange equation still can be employed to establish dynamic models for them.

5. Discussion and conclusion

In this work, we propose a new modeling approach to precisely describe the dynamic responses of the DEA-MES in a relative wide frequency range. To this end, we firstly investigate the dynamic responses of the DEA-MES under periodic exciting voltages and find that: (i) the dynamic responses show both viscoelastic creep and hysteresis effects; (ii) the hysteresis loops are both asymmetric and rate-dependent.

Then, the DEA-MES is equivalent to a slider-crank mechanism, where the stress distribution on the DEA-MES is calculated and viscoelastic nonlinearity is considered as a series of viscoelastic units. Based on the equivalent slider-crank mechanism, the Lagrange equation is introduced to develop an analytical dynamic model for the DEA-EMS. The effectiveness of the developed dynamic model is verified by the comparisons between the experimental data and predicted results. Considering that the dynamic model can accurately predict the dynamic response in a wide frequency range, it may pave the way for controller development. In addition, our dynamic model takes all the geometric parameters into consideration, which may be further used for optimization design of the DEA-MES in the future.

Acknowledgments

This work was supported in part by the National Natural Science Foundation of China under Grant 51622506 and Grant 51620105002, in part by the Science and Technology Commission of Shanghai Municipality under Grant 16JC1401000.

ORCID iDs

Guoying Gu https://orcid.org/0000-0002-0923-4319

References

[1] Kofod G, Wirges W, Paajanen M and Bauer S 2007 Energy minimization for self- organized structure formation and actuation *Appl. Phys. Lett.* **90** 081916
[2] Kofod G, Paajanen M and Bauer S 2006 Self-organized minimum-energy structures for dielectric elastomer actuators *Appl. Phys.* A **85** 141–3
[3] Araromi O, Gavrilovich I, Shintake J, Rosset S, Richard M, Gass V and Shea H 2015 Rollable multisegment dielectric elastomer minimum energy structures for a deployable microsatellite gripper *IEEE/ASME Trans. Mechatronics* **20** 438–46
[4] Shintake J, Rosset S, Schubert B, Floreano D and Shea H 2015 Versatile soft grippers with intrinsic electroadhesion based on multifunctional polymer actuators *Adv. Mater.* **28** 231–8
[5] Gu G, Zou J, Zhao R, Zhao X and Zhu X 2018 Soft wall-climbing robots *Sci. Robot.* **3** eaat2874
[6] Xu L, Chen H, Zou J, Dong W, Gu G, Zhu L and Zhu X 2017 Bio-inspired annelid robot: a dielectric elastomer actuated soft robot *Bioinspir. Biomim.* **12** 025003
[7] Cao J, Qin L, Liu J, Ren Q, Foo C, Wang H, Lee H and Zhu J 2018 Untethered soft robot capable of stable locomotion using soft electrostatic actuators *Extreme Mech. Lett.* **21** 9–16
[8] Li T, Li G, Liang Y, Cheng T, Dai J, Yang X, Liu B, Zeng Z, Huang Z and Luo Y 2017 Fast-moving soft electronic fish *Sci. Adv.* **3** e1602045
[9] Zhao J, Niu J, McCoul D, Leng J and Pei Q 2015 A rotary joint for a flapping wing actuated by dielectric elastomers: design and experiment *Meccanica* **50** 2815–24
[10] Zhao J, Wang S, McCoul D, Xing Z, Huang B, Liu L and Leng J 2016 Bistable dielectric elastomer minimum energy structures *Smart Mater. Struct.* **25** 075016
[11] Foo C C, Cai S, Koh S J A, Bauer S and Suo Z 2012 Model of dissipative dielectric elastomers *J. Appl. Phys.* **111** 034102
[12] Zhao X and Suo Z 2008 Method to analyze programmable deformation of dielectric elastomer layers *Appl. Phys. Lett.* **93** 251902
[13] O'Brien B, Gisby T, Calius E, Xie S and Anderson I 2009 FEA of dielectric elastomer minimum energy structures as a tool for biomimetic design *Electroactive Polymer Actuators and Devices (EAPAD) 2009. International Society for Optics and Photonics* **7278** 728706
[14] Samuel R, Oluwaseun A A, Jun S and Herbert S 2014 Model and design of dielectric elastomer minimum energy structures *Smart Mater. Struct.* **23** 085021
[15] Li W, Zhang W, Zou H, Peng Z and Meng G 2018 A fast rolling soft robot driven by dielectric elastomer *IEEE/ASME Trans. Mechatronics* **23** 1630–40
[16] Cao J, Liang W, Zhu J and Ren Q 2018 Control of a muscle-like soft actuator via a bioinspired approach *Bioinspir. Biomim.* **13** 066005
[17] Zhu J, Kollosche M, Lu T, Kofod G and Suo Z 2012 Two types of transitions to wrinkles in dielectric elastomers *Soft Matter* **8** 8840–6
[18] Godaba H, Zhang Z, Gupta U, Foo C and Zhu J 2017 Dynamic pattern of wrinkles in a dielectric elastomer *Soft Matter* **13** 2942–51
[19] Zou J, Gu G and Zhu L 2016 Open-loop control of creep and vibration in dielectric elastomer actuators with phenomenological models *IEEE/ASME Trans. Mechatronics* **22** 51–8
[20] Poulin A and Rosset S 2019 An open-loop control scheme to increase the speed and reduce the viscoelastic drift of dielectric elastomer actuators *Extreme Mech. Lett.* **7** 20–6
[21] Gu G, Gupta U, Zhu J, Zhu L and Zhu X 2017 Modeling of viscoelastic electromechanical behavior in a soft dielectric elastomer actuator *IEEE Trans. Robot.* **33** 1263–71
[22] Kao Chih-Cheng, Chuang Chin-Wen and Fung Rong-Fong 2006 The self-tuning PID control in a slider–crank mechanism system by applying particle swarm optimization approach *Mechatronics* **16** 513–22
[23] Rizzello G, Naso D, York A and Seelecke S 2015 Modeling, identification, and control of a dielectric electro-active polymer positioning system *IEEE Trans. Control Syst. Technol.* **23** 632–43
[24] Ogden Raymond W and Hill R 1972 Large deformation isotropic elasticity—on the correlation of theory and experiment for incompressible rubberlike solids *Proc. R. Soc.* A **326** 565–84